Pergamon

0306-4522(94)00283-5

Neuroscience Vol. 63, No. 1, pp. 207–221, 1994
Elsevier Science Ltd

0306-4522/94 $7.00 + 0.00

LOCALIZATION OF MUSCARINIC m3 RECEPTOR PROTEIN AND M3 RECEPTOR BINDING IN RAT BRAIN

A. I. LEVEY,*† S. M. EDMUNDS,† C. J. HEILMAN,† T. J. DESMOND‡ and K. A. FREY‡

†Department of Neurology, Emory University School of Medicine, Atlanta, GA 30322, U.S.A.
‡The Mental Health Research Institute, The University of Michigan, Ann Arbor, MI 48109, U.S.A.

Abstract—A family of receptor subtypes, defined either by molecular (m1–m5) or pharmacological (M1–M4) analysis, mediates muscarinic cholinergic neurotransmission in brain. The distribution and functions of the m3 receptor protein in brain and its relation to M3 ligand binding sites are poorly understood. To better characterize the native brain receptors, subtype-specific antibodies reactive with the putative third inner loops were used: (i) to measure the abundance of m3 protein and its regional distribution in rat brain by immunoprecipitation; (ii) to determine the cellular and subcellular distribution of m3 protein by light microscopic immunocytochemistry; and (iii) to compare the distribution of m3 immunoreactivity with the autoradiographic distribution of M3 binding sites labeled by [^{3}H]4-diphenylacetoxy-*N*-methyl piperidine methioxide in the presence of antagonists selective for the other receptor binding sites. The m3 protein, measured by immunoprecipitation, accounted for 5–10% of total solubilized receptors in all brain regions studied. Immunocytochemistry also revealed a widespread distribution of m3-like immunoreactivity, and localized the subtype to discrete neuronal populations and distinct subcellular compartments. The distribution of m3 protein was consistent with the messenger RNA expression, and like M3 binding sites, the protein was enriched in limbic cortical regions, striatum, hippocampus, anterior thalamic nuclei, superior colliculus and pontine nuclei. However, m3 immunoreactivity and M3 binding were differentially localized in regions and lamina of cortex and hippocampus.

The results confirm the presence of m3 protein in brain, its low abundance compared to other muscarinic receptor subtypes, and provide the first immunocytochemical map of its precise localization. The distribution of m3 suggests that it mediates a wide variety of cholinergic processes in brain, including possible roles in learning and memory, motor function and behavioral state control. However, since the distribution of the molecularly-defined receptor protein is distinct from the pharmacologically-defined M3 binding site, investigations of the functions of m3 in brain must await development of more selective ligands or use of non-pharmacological approaches.

Muscarinic acetylcholine receptor subtypes mediate diverse cholinergic effects in brain and other tissues. The subtypes are classified either pharmacologically by differential binding affinities for antagonists (M1–M4)[36] or genetically by direct sequence analysis (m1–m5).[2,11,26] The use of two classification schemes and a variety of methods for identification of receptor binding sites, mRNA and proteins have led to considerable uncertainty regarding the distributions and functions of the subtypes. A general correspondence between M1–M4 binding sites and the respective m1–m4 gene products (proteins) has been suggested,[8,11,22,39] based largely on the binding affinities of the cloned receptors. However, the subtypes have a high degree of sequence homology in the putative transmembrane domains where ligand binding occurs,[11] making development of more highly selective drugs for m1–m5 difficult.[4,6] For this reason, the relationships between native binding sites in brain and the molecularly distinguished proteins are uncertain.[16,19]

Methodological improvements for receptor localization, including autoradiography with more selective ligands and immunocytochemistry with subtype-selective antibodies, have begun to clarify the distributions of the subtypes and the degree of correspondence between the classification systems. M1 sites defined pharmacologically by high-affinity binding of pirenzepine and related compounds,[9,39] and m1 protein measured by immunoprecipitation,[16,19,37] are both present at highest levels in neocortex, hippocampus and striatum, with much lower levels in thalamus and other hindbrain structures. Immunocytochemical studies have recently localized m1 to postsynaptic sites on the somata and dendrites of most neurons in cortex, hippocampus and striatum.[10,16,24] M2 sites defined pharmacologically by low affinity with pirenzepine and high affinity with AF-DX 116 and other compounds,[11,36,39] and m2

*To whom correspondence should be addressed.

Abbreviations: AF-DX 116, 11-([2-{(diethylamino)methyl}-1-piperidinyl]acetyl-5,11-dihydro-6H-pyrido[2,3-b][1,4]-benzodizepine-6-on; 4-DAMP, 4-diphenylacetoxy-*N*-methylpiperidine methioxide; NMS, *N*-methylscopolamine; TE, Tris–EDTA buffer; TED, Tris–EDTA–digitonin buffer.

protein measured by immunoprecipitation[16,18] are both widespread in brain. Immunocytochemical studies have more precisely localized m2 to cholinergic and non-cholinergic neurons and both pre- and postsynaptic sites.[10,15,24] Although these comparisons show a general agreement in the distributions of M1 and m1, and M2 and m2, the other subtypes complicate this apparent correspondence. For example, the m4 protein is abundant in forebrain regions and likely contributes to both M1 and M2 binding sites.[16,35] Indeed, m3, m4 and m5 all have intermediate binding affinities for M1- and M2-preferring ligands,[4,6] and the distributions of the mRNA and/or proteins overlap with the other muscarinic proteins. Difficulty measuring and visualizing non-M1/M2 and non-m1/m2 subtypes by both autoradiography and immunocytochemistry has precluded further comparisons.

Recently, independent methods for localizing M3 binding sites and m3 receptor immunoreactivity have been developed. Zubieta and Frey[43] described receptor autoradiographic techniques using [^{3}H]4-DAMP in the presence of unlabeled pirenzepine and AF-DX 116 to visualize M3 binding sites selectively in a wide distribution in brain. Subtype-specific antibodies reactive with m3 protein have been developed in our laboratory[17] and others,[38] and although the protein has been detected by immunoprecipitation, the precise regional and cellular distribution of m3 in brain has not been described using immunocytochemical methods. The goals of the present study were to further investigate the distributions of m3 by immunoprecipitation and immunocytochemistry, and to compare these findings with the distribution of M3 binding sites.

EXPERIMENTAL PROCEDURES

Antibodies

Antisera and affinity-purified rabbit polyclonal antibodies reactive with the putative third intracellular loops of the m3 receptor were generated and characterized previously[16,17] This region is highly divergent among all muscarinic and other identified receptors. In specificity tests using the entire family of cloned receptors expressed in transfected mammalian cells, the antibodies are selective for the m3 protein by immunoprecipitation[16] and Western blot analysis.[10] Moreover, in specificity tests using native receptors expressed in tissues, the antibodies immunoprecipitate m3 receptors labeled with [^{3}H]*N*-methylscopolamine ([^{3}H]NMS,[5] and they also react with a single protein on immunoblots of brain membranes that corresponds to the size of the cloned protein.[10] Antisera selective for the other muscarinic receptor subtypes m1–m5 were also used for immunoprecipitation studies and were characterized in detail previously.[16]

Immunoprecipitation of solubilized muscarinic receptors

Muscarinic receptor subtypes were measured by immunoprecipitation[16] in dissected rat brain regions, including frontal cortex, hippocampal formation, caudate–putamen, thalamus and the ventral midbrain (including the substantia nigra). Ten male rats (Harlan Sprague–Dawley, Indianapolis, IN) were killed by decapitation, the brains were removed, dissected and then homogenized by hand in a glass homogenizer at 4°C in 10 volumes (w/v) of Tris–EDTA buffer (TE: 10 mM Tris, 1 mM EDTA, pH 7.5) additionally containing 0.2 mM phenylmethylsulfonyl fluoride, 1 μM pepstatin A, 1 μg/ml leupeptin and 10 μg/ml soybean trypsin inhibitor to retard proteolysis. Homogenates were centrifuged at 20,000 *g* for 10 min and the supernatant discarded. Pellets were resuspended in half the original volume of TE and aliquots were frozen at −70°C before receptor and protein assays. Individual homogenates consisted of pooled tissue from each of two brains to permit duplicate analyses of all samples. Receptors were solubilized by brief re-homogenization of pellet aliquots at 4°C in TE with added detergents (TED: TE buffer, additionally containing 0.4% digitonin and 0.04% cholic acid) at a final protein concentration of approximately 1 mg/ml. The homogenate was incubated at 4°C for 1 h, and then centrifuged at 12,000 *g* for 30 min. The total numbers of solubilized muscarinic receptors in the supernatants were determined by gel filtration as described below. For subtype immunoprecipitations, solubilized receptors were labeled with 10 nM [^{3}H]NMS (determined by saturation binding analysis to label the vast majority of solubilized receptors), and parallel samples were each mixed with a single antiserum specific for one of the m1–m5 receptors (final dilution 1:50) at 4°C for 4 h, and then goat anti-rabbit (final dilution 1:10) was added to a final volume of 285 μl and incubated overnight to co-precipitate immune complexes (containing rabbit anti-receptor–receptor-[^{3}H]NMS). The immunoprecipitates were pelleted by centrifugation (1000 *g*), washed rapidly by resuspension in ice cold TED buffer, recentrifuged and radioactivity in the pellets was determined by liquid scintillation spectroscopy. Control immunoprecipitates using non-immune sera or irrelevant antisera (reactive with dopamine receptor subtypes[15] and sodium–potassium ATPase) were performed in each assay to determine non-specific trapping of [^{3}H]NMS, and these values were subtracted from experimental samples.

Total muscarinic receptor binding in the homogenates was determined by membrane filtration assay after labeling in 1 nM [^{3}H]NMS (82 Ci/mmol) with 1 μM atropine sulfate to define non-specific binding, as described previously.[7] Total solubilized muscarinic receptors were determined in 125 μl aliquots of the supernatants, diluted in TED to a final volume of 2.5 ml. Routine assays of maximal binding capacity employed an incubation time of 6 h at 4°C in 10 nM [^{3}]NMS. This concentration was determined following saturation analyses that were conducted at ligand concentrations between 0.1 and 12.5 nM. Non-specific binding was determined in the additional presence of 1 μM atropine. Receptor-bound activity was determined by chromatography of duplicate samples using Sephadex G-25 columns with a 3 ml bed volume (Pharmacia Biotech Inc., Piscataway, NJ). Bound and free activities were eluted in successive 100 μl fractions of TED and were assayed by liquid scintillation spectroscopy. The peak of receptor-bound activity eluted at approximately 1 ml, and was quantified by integration of the nine fractions surrounding the peak. The peak of activity corresponding to free ligand eluted in fractions between 2.5 and 3 ml of added TED. Saturation of NMS binding to solubilized receptors was analysed with the Ligand Program for computer-assisted, non-linear curve-fitting.[25] Solubilization efficiency was defined as the ratio of specific NMS binding in solubilized supernatants to specific NMS binding in the original homogenates. Protein was determined with the bicinchoninic acid method.[31]

Immunocytochemistry

Nineteen male albino rats (Charles River) were deeply anesthetized with chloral hydrate, perfused intracardially with 0.9% saline, followed by 0.1 M phosphate-buffered 3% paraformaldehyde, pH 7.4, and then 10% buffered sucrose.

One animal was fixed with 2% paraformaldehyde, 0.05 M lysine and 0.005 M sodium periodate. Brains were immediately removed, placed in 30% buffered sucrose for several days, frozen on dry ice and sectioned at 40 μm on a sliding microtome. Tissue sections were processed for immunocytochemistry using the avidin–biotin–peroxidase method (Elite, Vector Labs), and developed with diaminobenzidine hydrochloride as described previously.[16] Some sections from two rats were pretreated with hydrogen peroxide and sodium hydroxide to quench endogenous peroxidase and enhance antigen retrieval as described.[30] Affinity-purified antibodies to m3 were used at a final concentration of 0.5–1.0 μg/ml; this dilution was chosen to optimize the signal-to-noise ratio. Immunocytochemical controls consisted of adsorption of the receptor antibodies with 100 μg/ml of immobilized-GST or m3i3-GST fusion proteins, and omission of the primary antibody.

Autoradiographic ligand binding studies

Three male rats (Harlan Sprague–Dawley, Indianapolis, IN) were killed by decapitation, and the brains rapidly removed and frozen in crushed dry ice. Specimens were covered with embedding medium (Lipshaw, Detroit, MI) and stored at −70°C. Quadruplicate, coronal brain sections (20 μm) were obtained with the use of a cryostat microtome at −18°C. Two adjacent sections at each level were mounted on each of two gelatin-subbed microscope slides, thaw-mounted and allowed to dry at room temperature. Slides were then stored at −70°C until use in binding assays. Autoradiographic binding assays were performed as described previously.[43] Slides were washed in buffer to remove endogenous interfering substances, incubated in the presence of 5 nM[^{3}H]4-DAMP (82.6 Ci/mmol) for 60 min to label muscarinic receptors, followed by two successive 1 min incubations in fresh buffer at 4°C to remove non-specific binding. Slides were then dipped briefly in cold distilled water to remove excess buffer salts and allowed to air-dry. At each anatomic level, one slide was prepared for evaluation of total 4-DAMP binding, as described above, while the second slide was processed to enhance the relative contribution of M3 receptors. This was accomplished by the addition of 1 μM concentrations of unlabeled AF-DX 116 and pirenzepine to the [^{3}H]4-DAMP incubation. This protocol results in 95% reductions in the binding of 4-DAMP to M1 and M2 receptors, while labeling 40% of the M3 receptors; in a hypothetical region containing equal admixtures of M1, M2 and M3 receptors, 85% of 4-DAMP binding under these conditions is attributable to the M3 sites. Autoradiograms were generated by apposition of slides to tritium-sensitive X-ray film (Hyperfilm-3H, Amersham, Arlington Heights, IL) for four weeks. Autoradiographic images were analysed with the use of a computer-assisted video densitometer (MCID system, Imaging Research, St Catherines, Ontario).

Materials

AF-DX 116 and pirenzepine were the generous gift of Dr Karl Thomae, Gmbh, Beberach an der Riss, Germany. [^{3}H]4-DAMP and [^{3}H]NMS were purchased from New England Nuclear (Boston, MA). Atropine sulfate was obtained from Sigma Chemical Co. (St Louis, MO).

RESULTS

Immunoprecipitation assay of muscarinic receptors

Saturation analyses of [^{3}H]NMS binding to solubilized muscarinic receptors from whole brain were consistent with a homogeneous population of binding sites in each of three independent assays when analysed individually, and again in combination

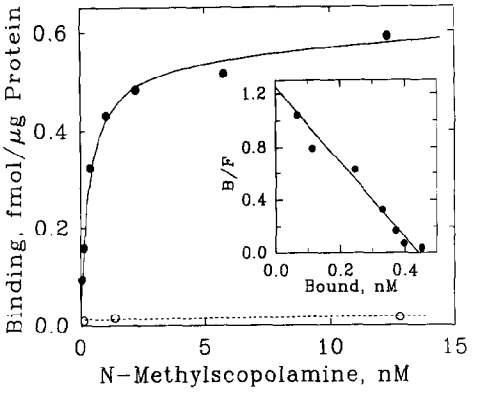

Fig. 1. Binding of [^{3}H]NMS to solubilized muscarinic receptors from rat brain. Aliquots of solubilized receptors were incubated in the presence of varying concentrations of [^{3}H]NMS, and bound activity separated by Sephadex gel chromatography. Total binding (solid line, closed circles) and non-specific binding (dashed line, open circles) as estimated in the presence of 1 μM atropine are depicted from one of three independent experiments. Inset: Scatchard (Rosenthal) plot of specific NMS binding. The data are consistent with ligand binding to a homogeneous receptor population.

(Fig. 1). The estimated equilibrium dissociation constant was 0.30 ± 0.03 nM (mean ± S.D.), with Hill coefficients ranging between 0.85 and 0.96. On this basis, 10 nM [^{3}H]NMS was chosen to provide essentially complete saturation of solubilized receptors for immunoprecipitation studies. This concentration of radioligand resulted in somewhat higher but acceptable levels of background compared to previous studies using 1 nM [^{3}H]NMS,[16] with non-specific trapping of [^{3}H]NMS averaging 19% of total specific solubilized receptors added to each assay (ranging from 13% in striatum to 23% in ventral midbrain). There were no significant differences in background levels with non-immune sera or different control antisera to dopamine receptors and other brain proteins. This indicates that variations in the immunoglobulin concentrations as occurs among different antisera do not influence recovery of muscarinic receptor subtypes.

Other factors potentially affecting the immunoprecipitation assay were also analysed. Dissociation of [^{3}H]NMS from receptors during the immunoprecipitation process might occur due to antibody binding, washing or other reasons. To test these possibilities, solubilized receptors were incubated in [^{3}H]NMS, followed by determination of bound activity by gel filtration. Addition of specific antisera or 10 μM atropine for up to 60 min following the labeling of receptors did not reduce the recovery of specifically-bound activity as determined by gel filtration. Thus, it is unlikely that appreciable amounts of NMS dissociate during the immunoprecipitation procedure. Since solubilization efficiencies averaged 49%, we also investigated the possible fate of muscarinic receptors identified in the initial

Table 1. Regional analysis of m3 protein in rat brain by immunoprecipitation

Region	n	Specific binding* (d.p.m.)	Percentage m3†	m3‡ (pmol/mg)
Frontal cortex	5	3783 ± 563	7 ± 4	0.08 ± 0.04
Hippocampus	5	3559 ± 280	7 ± 2	0.07 ± 0.01
Striatum	5	8700 ± 703	5 ± 1	0.09 ± 0.01
Thalamus	5	3223 ± 122	8 ± 3	0.04 ± 0.01
Midbrain	5	1412 ± 200	12 ± 6	0.04 ± 0.02

*Total specific binding of [^{3}H]NMS to soluble receptors was determined by gel filtration. Non-specific binding was determined in the presence of 1 μM atropine and subtracted from total binding. Values reflect the mean and standard deviation of five independent assays, each conducted on tissues pooled from two animals.

†Values shown are the percentage of total solubilized [^{3}H]NMS binding sites recovered in immunoprecipitates with m3 antisera minus control immunoprecipitates using irrelevant antisera.

‡Corrected for solubilization efficiency (see Experimental Procedures), total binding and [^{3}H]NMS specific activity (180.93 d.p.m./fmol).

tissue homogenates, but not accounted for in assays of solubilized sites. Repeated detergent exposure of the residual unsolubilized tissue pellet did not result in additional solubilized binding sites. Neither did membrane filtration binding assays detect the presence of residual receptors in the post-detergent pellet, suggesting that receptors not represented in the detergent supernatants are denatured during the solubilization procedure.

Immunoprecipitation of m3 in rat brain

Immunoprecipitation studies were used to determine the abundance of m3 receptor in various regions of rat brain, as shown in Table 1. Precipitation of this subtype accounted for 5–12% of the total number of solubilized [^{3}H]NMS binding sites. Although these levels were relatively low, the immunoprecipitates with m3 antisera yielded significantly greater [^{3}H]NMS recovery than control precipitates using non-immune sera for every region ($P < 0.05$, Student's t-test). The smallest relative difference between m3 and control immunoprecipitates was in frontal cortex (m3 was 21% higher than controls) and the largest difference in ventral midbrain (m3 was 53% higher than controls). As mentioned above, the use of different control antisera did not influence the results. The distribution among dissected regions was also fairly uniform, with estimates of the tissue densities (corrected for solubilization efficiencies) ranging from 0.04 pmol/mg membrane protein in midbrain and thalamus to 0.09 pmol/mg in striatum.

The composition and relative abundance of the entire family of muscarinic receptors in rat brain are shown in Table 2. Recovery of muscarinic receptor subtypes was close to 100%, based on the sum of the immunoprecipitates. In frontal cortex and hippocampus, m1, m2 and m4 were the most abundant subtypes and each accounted for roughly one-quarter to one-third of the total population of solubilized [^{3}H]NMS binding sites. In striatum, the m4 subtype alone accounted for nearly one-half of the total receptors, whereas in thalamus and midbrain m2 was the most abundant subtype. The m5 receptor was recovered at low levels in every brain region, and was statistically significant compared to controls ($P < 0.05$) in every case except in ventral midbrain.

Light microscopic distribution of m3 immunoreactivity in rat brain

The immunocytochemical distribution of m3 was widespread in rat brain, as shown in the right column of Fig. 2. In general, the microscopic appearance of the diaminobenzidine peroxidase reaction product was brown and finely granular, and associated with cell bodies, neuritic processes and neuropil. The density of the reaction product was routinely much less than as described previously for m1, m2 and m4.[16] Sections pretreated with hydrogen peroxide and sodium hydroxide exhibited moderately improved sensitivity compared to untreated sections. Immunological specificity was demonstrated by inhibition of staining after preadsorption of the antisera with

Table 2. Distribution of m1–m5 in rat brain by immunoprecipitation*

Region	m1	m2	m3	m4	m5	Sum
Frontal cortex	25 ± 4	36 ± 11	7 ± 4	29 ± 4	6 ± 4	104 ± 14
Hippocampus	38 ± 9	21 ± 5	7 ± 2	21 ± 3	6 ± 2	94 ± 12
Striatum	27 ± 1	12 ± 1	5 ± 1	48 ± 2	5 ± 1	97 ± 3
Thalamus	8 ± 4	48 ± 5	8 ± 3	30 ± 7	6 ± 2	99 ± 11
Midbrain	10 ± 9	54 ± 7	12 ± 6	13 ± 3	6 ± 5	96 ± 7

*Shown are the percentage of total soluble receptors for each subtype ± S.D. Total soluble receptors and number of animals for each region as shown in Table 1.

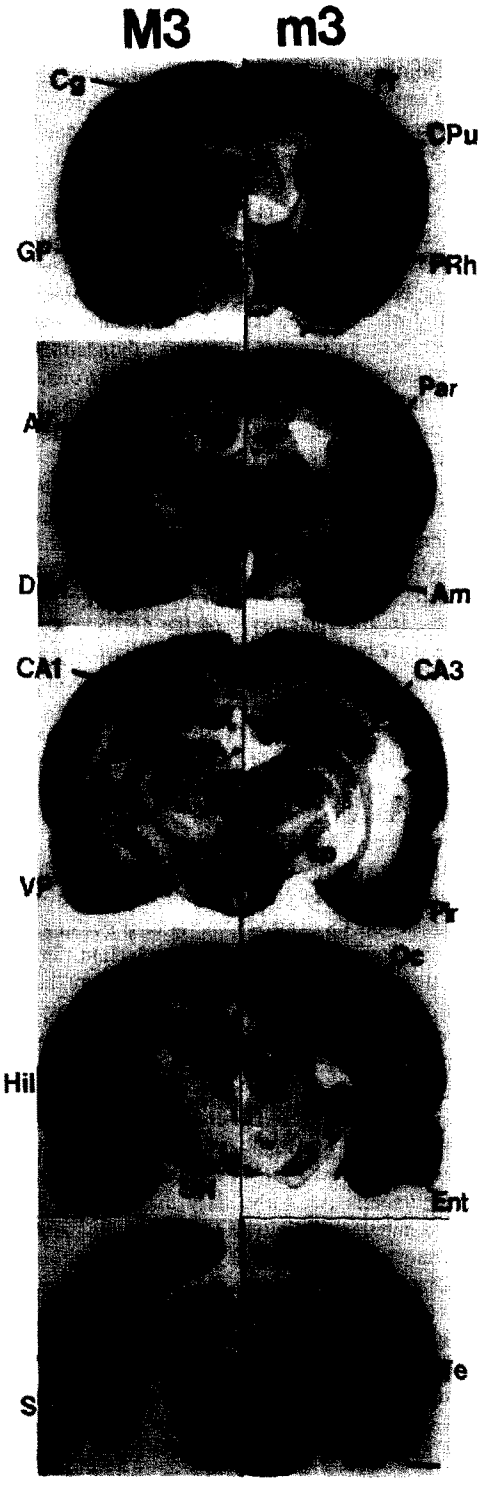

Fig. 2. Comparison of the distribution of M3 binding and m3 immunoreactivity in rat brain. Coronal sections were processed for visualization of M3 binding sites (left) with [^{3}H]4-DAMP plus unlabeled pirenzepine and AF-DX 116, and aligned with sections from separate animals processed for m3 immunoreactivity (right). The two markers show similar localization in most brain regions. Am, amygdala; Aq, aqueduct; AV, anteroventral thalamic nucleus; CA1 and CA3, fields of hippocampus; cc, corpus callosum; Cg, cingulate cortex; CPu, caudate-putamen; cp, cerebral peduncle; DEn, deep endopiriform cortex; Ent, entorhinal cortex; Fr, frontal cortex; GP, globus pallidus; Hil, hilus; Hy, hypothalamus; IC, inferior colliculus; MG, medial geniculate; Oc, occipital cortex; Par, parietal cortex; Pir, piriform cortex; Pn, pontine nuclei; PRh, perirhinal cortex; Rs, retrosplenial cortex; S, subiculum; SC, superior colliculus; SN, substantia nigra; Te, temporal cortex; VP, ventroposterior thalamic nucleus. Scale bar = 1 mm.

the i3 loop fusion protein. Control sections with omission of m3 antibody were routinely performed and showed light diaminobenzidine reaction product in occasional glia, select neurons and a few other structures that in most cases were easily distinguished from antibody-treated sections; exceptions will be further described. Glial immunoreactivity with m3 antibody was frequently detected, but because this staining was usually light and occasionally present in control sections, it is difficult to be certain if this represented specific reaction product. The same is true of blood vessels, which were frequently associated with immunoreactive fibers. Other descriptions of m3 immunoreactivity refer to specific staining not observed in controls, with the intent that the term denotes m3 "like" immunoreactivity. As with any immunocytochemical procedure, it is not possible to be certain that the reaction product is localized only to the m3 receptor in tissue sections, despite rigorous characterization of antibody specificity by immunoprecipitation and immunoblotting.

Cortical and related structures. In the olfactory bulb, m3 immunoreactivity was enriched diffusely in the glomeruli and moderately in the external plexiform layer. In the cerebral cortex, m3 immunoreactivity was differentially distributed across regions and lamina (Figs 2, 3). Limbic regions exhibited highest levels in cortex, including cingulate (Fig. 3D), retrosplenial, piriform (Fig. 3E), entorhinal (Fig. 4), and insula and deep endopiriform cortex in the perirhinal region (Fig. 2). Immunoreactivity was most dense in the neuropil in the superficial aspect of the molecular layer, and in neurons and the neuropil in layers II/III and V (Fig. 3). Some astroglial processes also appeared lightly stained (see above). Neuropil immunoreactivity was mostly diffuse, but also associated with fine neurites and puncta. In the hippocampal formation, entorhinal cortex (particularly layer II cell islands and layer V neurons/neuropil) and subiculum were prominently stained. In hippocampus proper, cell bodies and proximal dendrites of many pyramidal neurons and occasionally interneurons were lightly immunoreactive, with more intense diffuse and punctate immunoreactivity in the neuropil in the stratum lacunosum moleculare, deep aspects of the stratum radiatum and stratum oriens, with CA3 greater than CA1 (Fig. 4). In the dentate gyrus, neuropil immunoreactivity was most dense in the superficial molecular layer and the hilus, with little immunoreactivity in the granule cells. Amygdala nuclei with the most dense m3 immunoreactivity were the basolateral and central nuclei (Fig. 3F).

Subcortical forebrain structures. The striatum displayed among the highest densities of m3 immunoreactivity in brain (Figs 2, 3F). Diffuse and finely punctate neuropil immunoreactivity were present throughout dorsal striatum, nucleus accumbens and olfactory tubercle, and in some cases appeared patchy. Striatal neurons were rarely stained, and then only very lightly. In the basal forebrain (Fig. 4D), immunoreactive neurons, proximal processes and puncta were present in the medial septum, nuclei of the diagonal band of Broca, ventral pallidum, preoptic nuclei and nucleus basalis. While many of the large basal forebrain neurons were also lightly stained in control sections (Fig. 4E), m3-treated sections consistently yielded more intense staining of these neurons. The dorsolateral septum had diffuse neuropil m3 immunoreactivity. The globus pallidus, entopeduncular nucleus and substantia nigra contained abundant neurites and puncta, and also scattered neurons that were lightly stained. Subthalamus neurons were enriched in m3 immunoreactivity compared to most other basal ganglia nuclei (Fig. 5E).

Diencephalon. The anteroventral, anteromedial and anterodorsal nuclei displayed the most intense m3 staining among thalamic nuclei and possibly other brain regions (Fig. 5A). Neurons were prominent in the anterodorsal nucleus and the medial aspect of the anteroventral nucleus, while dense punctate immunoreactivity was observed in the lateral aspect of the anteroventral nucleus. Moderate levels of cellular immunoreactivity were present in lateral and medial geniculate, ventrobasal, mediodorsal, laterodorsal, lateroposterior, gelatinosus, reuniens, paraventricular and intralaminar nuclei. In some cases, remarkably large immunoreactive puncta were abundant in the lateral geniculate (Fig. 5D), ventrobasal and other nuclei; these profiles were often associated with the margins of cell bodies and rarely appeared as varicose swellings along axons. In the epithalamus and pretectum, immunoreactivity was present in neurons in lateral habenula, but not medial habenula, and also relatively intense in cells in the olivary pretectal nucleus and diffusely in the anterior pretectal nucleus (Fig. 5B). In the hypothalamus, most regions were more lightly stained than thalamus, with the exception that high levels of m3 immunoreactivity were present in neurons in the lateral mammillary nucleus (Fig. 5F) and in neuropil in the premammillary nucleus, and moderate levels were present in neurons in the paraventricular nucleus, lateral hypothalamus and diffusely in the ventromedial nucleus. Neurons in the zona incerta were also immunoreactive.

Brainstem. Because the hindbrain regions exhibited generally higher levels of background staining than in forebrain, uncertainty exists regarding many nuclei. The background staining was not due to m3 antibody, since it occurred in the controls even when the primary antibody was omitted. The following structures were none the less consistently enriched in m3 immunoreactivity compared to controls, and the possibility that other nuclei express low levels of m3 immunoreactivity cannot be dismissed. Immunoreactivity in the midbrain was localized to a dense plexus of fibers and puncta in the neuropil in the superficial layer of superior colliculus, and to more

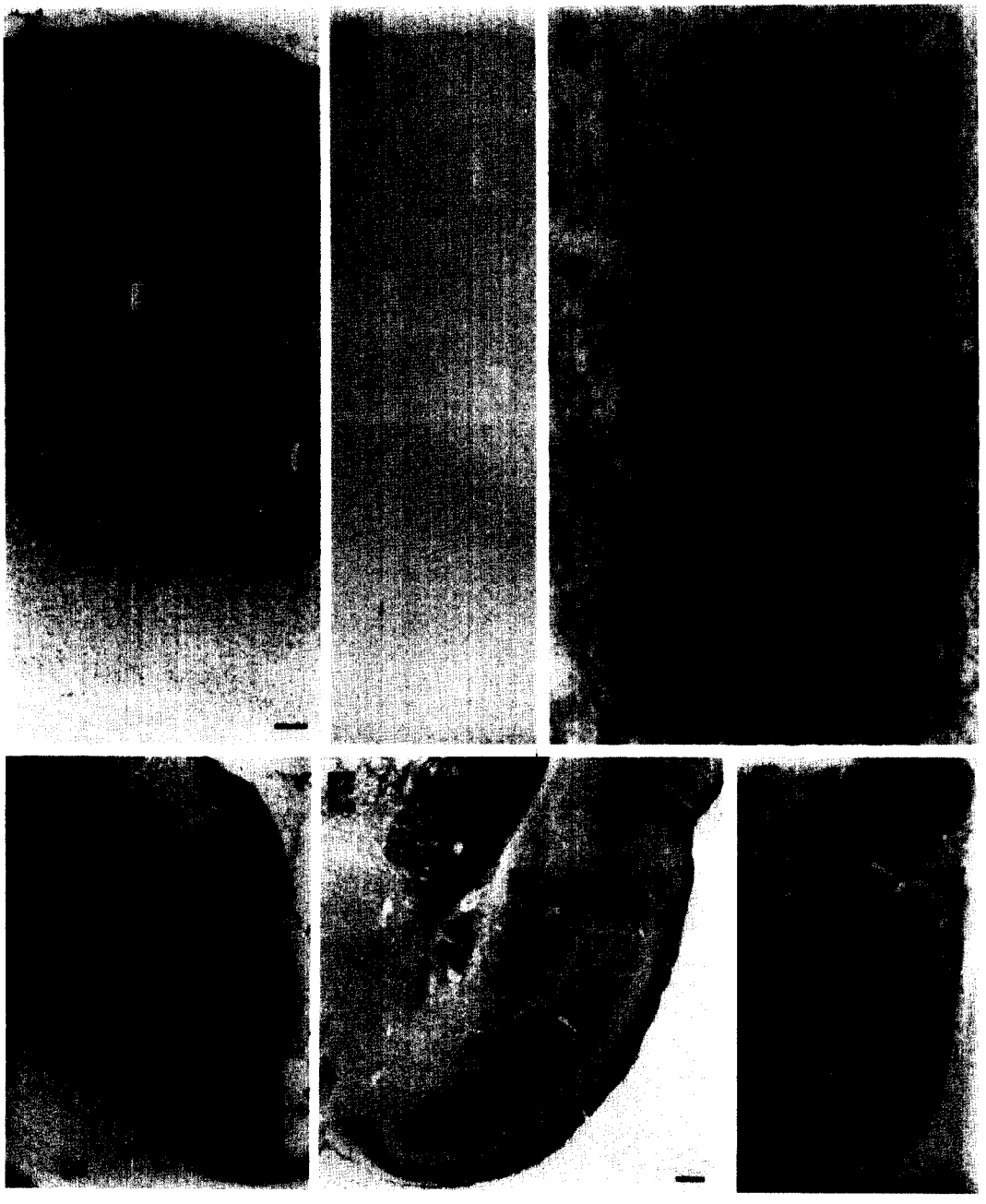

Fig. 3. Immunocytochemical localization of m3 in cortex and amygdala. (A) m3 immunoreactivity in frontal cortex; note the relatively enriched staining of the neuropil in the outer molecular layer (I) and layers II–III, and in pyramidal neurons in layer V. (B) Control with omission of m3 antibody. (C) Higher magnification of m3 immunoreactivity in layer V cortical neurons, proximal dendrites, and frequent neuritic processes and puncta. (D) Cingulate cortex is enriched in m3 immunoreactivity compared to adjacent motor cortical areas, but the laminar distribution is similar. Note low level of background in corpus callosum (cc). (E) Piriform (Pir) and deep endopiriform (DEn) cortex exhibit enriched m3 immunoreactivity. As in other cortical areas, note the increased staining of superficial molecular layer (arrow). (F) Amygdala nuclei show m3 immunoreactivity, including basolateral nucleus (BLA) and central nucleus (Ce). The caudate–putamen (CPu) is also enriched in m3 immunoreactivity (also shown in upper left of panel E). Scale bars = 100 μm (A, B); 25 μm (C); 200 μm (D–F).

weakly stained neuropil in deeper layers extending to the central gray (Fig. 6C). In the pontine nuclei (Fig. 6A, B), neurons and neuropil were both densely immunoreactive, and scattered neurons throughout the reticular formation were more darkly stained than in controls. In cerebellum, medulla and spinal cord,

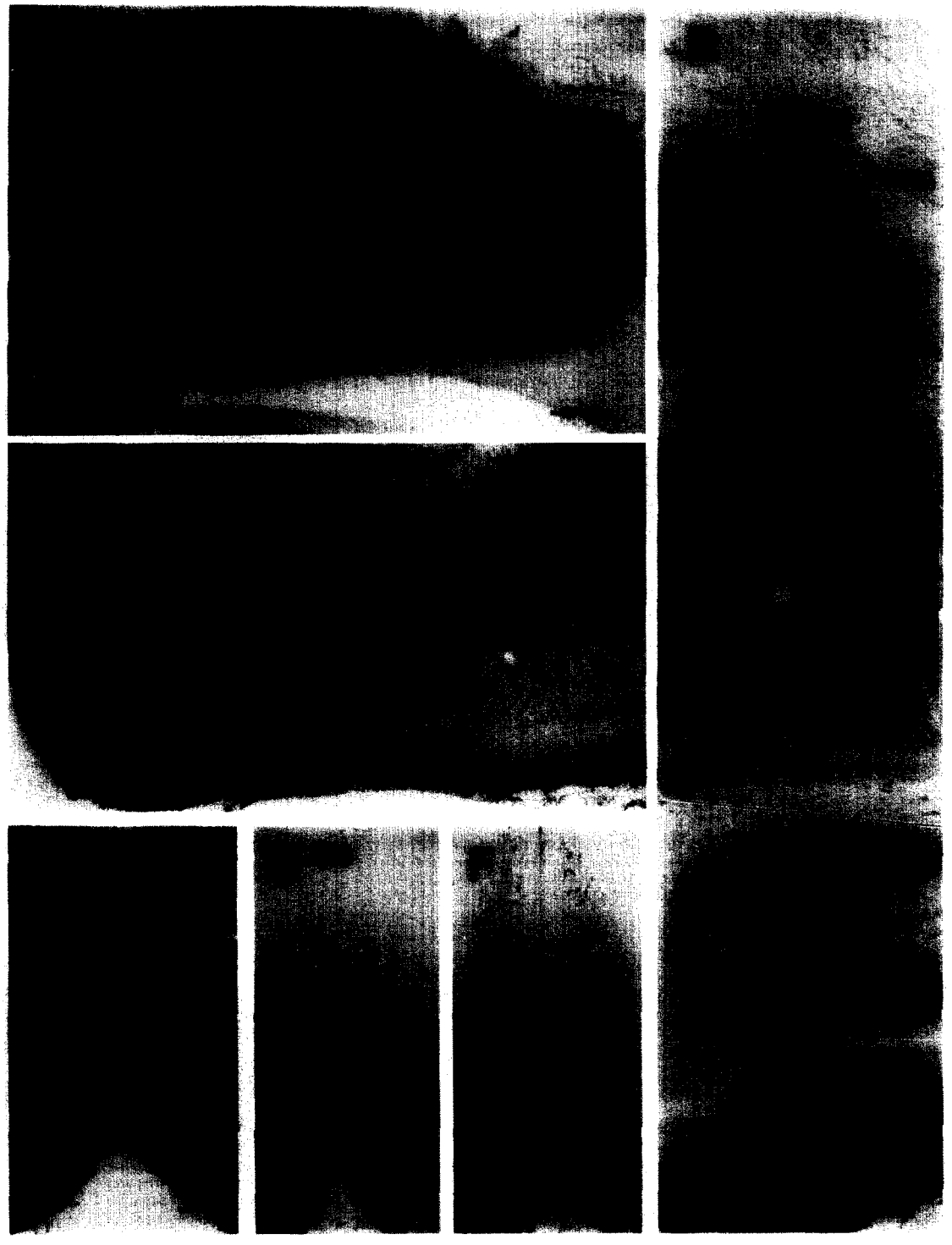

Fig. 4. Immunocytochemical localization of m3 in the hippocampal formation and medial septum. (A) Coronal section of hippocampus shows m3 immunoreactivity enriched in the CA3 neuropil compared to CA1, and also in the dentate gyrus (DG). (B) Higher magnification of m3 in CA1 and dentate gyrus is shown in this photomontage. Note the laminar patterns with immunoreactivity localized in cell bodies of pyramidal neurons (p), and relatively dense reaction product in the neuropil in the deeper aspects of the stratum radiatum (r), stratum lacunosum moleculare (l-m) and stratum oriens (o). The dentate gyrus, shown below the hippocampal fissure (dashed line), also expresses dense m3 immunoreactivity. Granule cells (gc) express low levels of m3, but the receptor is present in the neuropil in the molecular layer (mo) and hilus (hi) and occasional non-pyramidal neurons (arrow). (C) The entorhinal cortex expresses relatively high levels of m3 immunoreactivity compared to other cortical regions. The receptor is enriched in the superficial molecular layer, stellate neurons in layer II, and both neurons and neuropil in deep layers. (D–F) Coronal sections through the medial septum (MS) and diagonal band of Broca (DB), processed for m3 immunoreactivity (D), control (E) or choline acetyltransferase immunoreactivity (F).[14] Note the similar distributions of m3 immunoreactivity and cholinergic neurons, although the neuropil is more immunoreactive with the m3 antibody. The control section was processed without primary antibody, and shows low levels of background staining in many neurons. Scale bars = 200 μm (A–E).

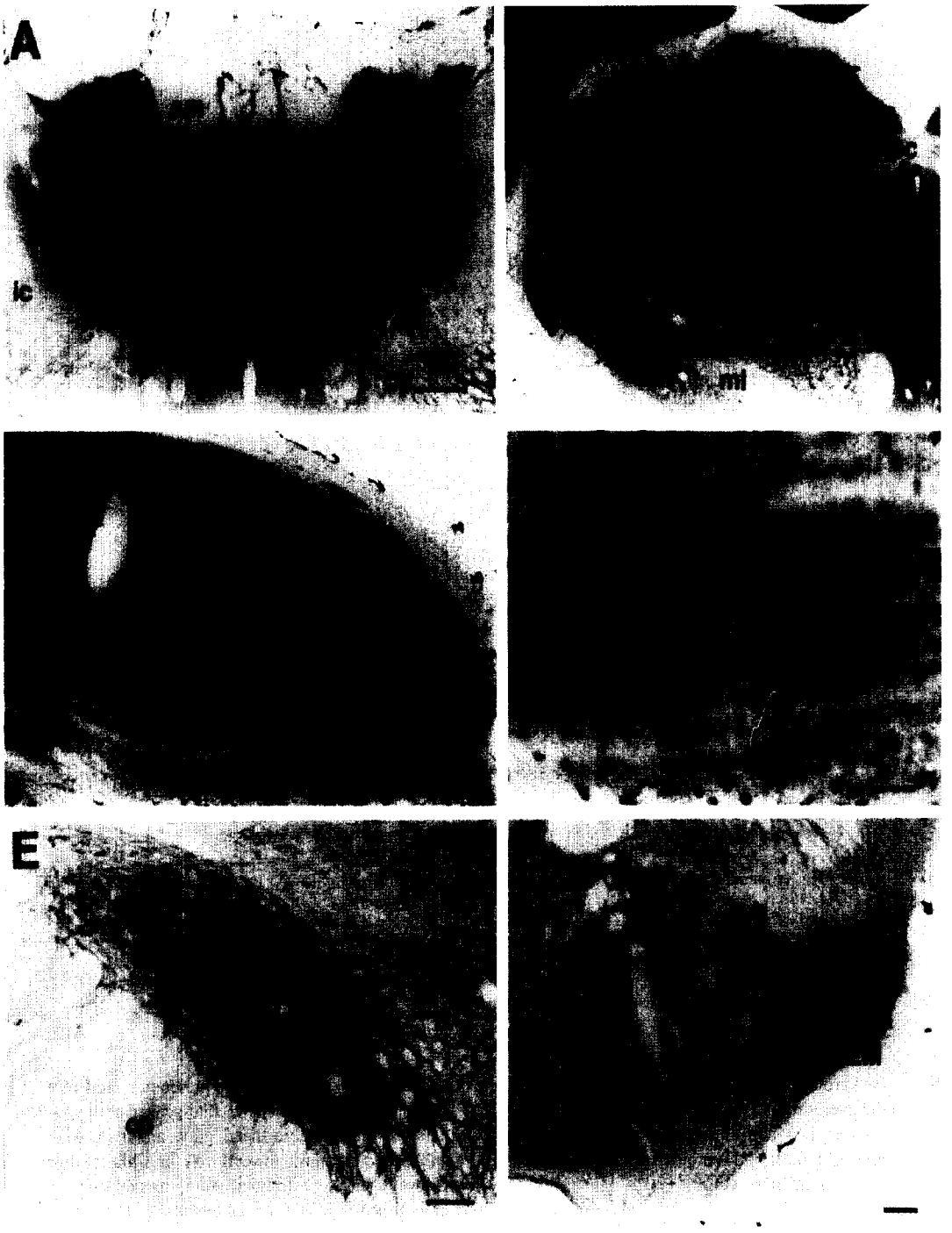

Fig. 5. Immunocytochemical localization of m3 in diencephalon. (A) Rostral thalamus shows highly enriched immunoreactivity, particularly in the anterior nuclear group (anterodorsal, AD, and anteroventral, AV), the midline nuclei (paraventricular, PV, and reuniens, Re) and reticular nucleus (Rt). (B) Caudal thalamic nuclei express moderate levels of m3 immunoreactivity, including dorsal lateral geniculate (LG) and lateral posterior (LP) nuclei. In pretectum, anterior pretectal (APT) and olivary pretectal (OPT) nuclei also express m3. (C, D) Higher magnification photomicrographs of lateral geniculate show m3-immunoreactive neurons and neuropil. The neurons are occasionally associated with dense punctate immunoreactivity at the margins of the cell body (arrows). (E) Subthalamic nucleus (STN) is enriched in m3 immunoreactivity compared to other basal ganglia structures other than striatum. (F) In hypothalamus, the lateral mammillary (LM) neurons and neuropil show high levels of m3 immunoreactivity, with low levels in the medial mammillary nucleus (MM). Note that white matter tracts in all sections show little or no immunoreactivity, including stria medullaris (sm), internal capsule (ic), medial lemniscus (ml), posterior commissure (pc) and cerebral peduncle (cp). Scale bars = 500 μm (A, B); 250 μm (C); 50 μm (D); 100 μm (E, F).

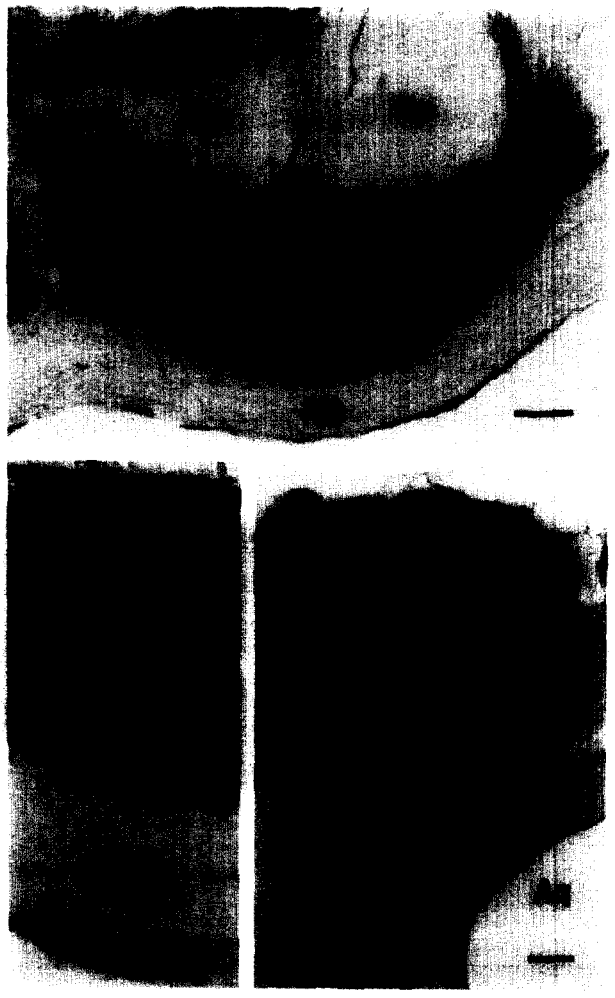

Fig. 6. Immunocytochemical localization of m3 in the pons and midbrain. (A) Pontine nuclei express relatively high levels of m3. (B) Higher magnification of pontine nuclei shows expression in cell bodies and diffusely in the neuropil. The low levels of staining in the cerebral peduncle were similar to controls. (C) The superficial layer of the superior colliculus (SC) expresses dense m3 immunoreactivity in the neuropil, with moderate levels in a patch (arrowheads) in deeper layers extending into the periaqueductal gray (PAG). Aq, aqueduct; cp, cerebral peduncle; lfp, longitudinal fasciculus pons; ml, medial lemniscus; PN, pontine nuclei; tfp, transverse fibers pons. Scale bars = 200 μm (A, C); 50 μm (B).

background staining was too high to evaluate, with the exception of the spinal trigeminal nucleus, which was enriched in fine fibers, and neurons in the cranial and spinal somatic motor nuclei also appeared weakly immunoreactive.

Comparison of m3 immunoreactivity and M3 binding

The regional distributions of m3 immunoreactivity and M3 binding to [^{3}H]4-DAMP (in the presence of pirenzepine and AF-DX 116) were compared in matched sections from different animals (Fig. 2). Results of M3 binding were described in detail previously and are uncorrected for tritium quenching.[43] The general distributions of both markers were similar, with relatively dense levels of staining or binding in neocortex, hippocampus, striatum, anterior thalamic nuclei, superior colliculus and pontine nuclei. Also, the markers were both present at moderate levels in lateral geniculate, medial geniculate, hypothalamus and periaqueductal gray, and they were both found at much lower levels in white matter pathways, such as corpus callosum, internal capsule, cerebral peduncle and medial lemniscus. There were also some significant differences in the distributions of m3 immunoreactivity versus M3 binding. For example, frontoparietal cortex was relatively enriched in M3 binding compared to the adjacent cingulate cortex, while the opposite pattern was found with m3 immunoreactivity. Also, laminar differences were marked in hippocampus, where M3 was most dense in stratum oriens and stratum radiatum of CA1 with little binding in CA3, while m3 immunoreactivity was most dense in the stratum lacunosum moleculare and deep radiatum of CA3. However,

minute comparisons were not attempted because of inherent limitations such as use of different animals for each marker (because of the need to use unfixed tissue for autoradiography and fixed tissue for immunocytochemistry), and likely differences in sensitivity and spatial resolution attainable with each method.

DISCUSSION

There are several principal findings of the present study. First, the low levels of m3 muscarinic acetylcholine receptor protein in widespread regions of rat brain have confirmed earlier immunoprecipitation studies. Second, the light microscopic immunocytochemical findings also demonstrate a wide distribution of m3 immunoreactivity, and indicate that the protein is localized in specific cells and subcellular sites, complementing and extending previous studies of m3 mRNA. Third, the general distributions of m3 receptor protein visualized by imunocytochemistry and M3 binding sites by autoradiography are similar but not identical, indicating that the two markers may not be equivalent. The findings clarify the localization of m3 receptor, its correspondence to the pharmacologically defined binding site, and suggest a variety of functional implications for m3 in muscarinic cholinergic neurotransmission in the central nervous system.

Abundance of m3 and other muscarinic receptor proteins in rat brain

Immunoprecipitation studies have been used to determine the proportion of m3 and other muscarinic receptor subtypes in dissected regions of rat brain. In our previous studies using 1 nM [^{3}H]NMS to label solubilized receptors, we were unable to recover significant levels of m3.[16] In the present study, saturation binding analysis using the native brain receptor population demonstrated an equilibrium dissociation constant of 0.30, suggesting that solubilized receptors were incompletely (about 75%) labeled by 1 nM [^{3}H]NMS. Indeed, using higher concentrations of ligand (10 nM) we now recover m3 in widespread regions of brain. Our results indicate that m3 is present at low levels, accounting for only about 5–10% of the total population of muscarinic receptors solubilized in the regions studied. However, we are cautious about interpreting these values, because despite their statistical significance, they are only about 20–50% greater than control immunoprecipitates due to the higher levels of background with 10 nM [^{3}H]NMS. The values more accurately reflect the upper limits of m3 contribution, given the saturating ligand concentration employed and the quantitative recovery of the receptors. None the less, our findings are in excellent agreement with immunoprecipitation studies of Wall *et al.*[38] using a peptide antibody directed to the C-terminus of m3. Potentially, methodological problems could result in apparently lower levels of m3 than are actually present in tissues. For instance, reduced solubilization of m3 compared to other subtypes (e.g. due to possible differential subcellular compartmentation) or loss of antigenic sites (e.g. due to proteolytic cleavage or post-translational modifications) are theoretically possible. However, radioligand binding studies using tissue homogenates and sophisticated kinetic analyses,[36] and autoradiographic binding studies[43] both generally agree with immunoprecipitation studies, and neither approach depends on solubilization of receptors. Also, since our polyclonal antibodies are directed to a variety of epitopes on the large i3 loop, and the polyclonal antibodies of Wall *et al.*[38] recognize the C-terminus, loss of both of these antigenic regions is unlikely.

Improved recovery of m3 in our immunoprecipitation assay using 10 nM [^{3}H]NMS prompted a reanalysis of the entire family of m1–m5 receptors using a panel of subtype-specific antibodies (Table 2). Contributions of m1 and m2 receptors to the total receptor populations were comparable to the results of our previous immunoprecipitation studies,[16] as well as those of Wolfe and colleagues.[18,37] However, the levels of m4 in each region are about 15% higher than we found previously, suggesting that this subtype was incompletely labeled with lower concentrations of radiolabel. The m4 receptor now appears to be the predominant subtype in striatum and accounts for almost a third of the total muscarinic receptors in cortex and thalamus. These results are in excellent agreement with other recent immunoprecipitation studies.[42] The m5 receptor also appeared to be recovered more efficiently in the present study, although present at very low levels throughout the brain. As discussed above for m3, we are unsure about the lower limits of measurable m5 receptors and the meaningfulness of these results. Our upper limit estimates of 5–6% of total receptors in each region are somewhat higher than the levels of m5 reported by Yasuda *et al.*[42] (<2%) using different antibodies and techniques. The widespread distribution of m5 protein is somewhat surprising, given the limited distribution of m5 mRNA found by *in situ* hybridization studies.[34,41] However, differences in the sensitivity of the methods may explain this mismatch, since m5 mRNA is detectable throughout the brain using more sensitive polymerase chain reaction methods.[40] Other possible explanations are differences in turnover, stability or subcellular distribution of the mRNA versus protein. Direct localization of m5 receptor protein will be necessary to address these issues, although our attempts using immunocytochemistry have not been successful and specific ligands for autoradiographic binding are not available.

Immunocytochemical localization of m3

Antibodies specific to m3 have provided the first opportunity to determine the precise distribution

of this subtype using immunocytochemistry. The expression of m3 is widespread, consistent with the immunoprecipitation studies. The cellular localization of m3 protein also agrees well with *in situ* hybridization studies of m3 mRNA, including a close match in olfactory bulb, regions and layers of the cortex, hippocampal formation, thalamic nuclei, subthalamus, posterior hypothalamus, superior colliculus, central gray and pontine nuclei.[3] Although m3 mRNA is expressed in widespread regions of the brainstem, we are unsure of the distribution of protein because of problems with higher levels of background immunoreactivity in the hindbrain. The agreement between immunocytochemical and *in situ* hybridization approaches substantiates the distribution of m3, and implicates this subtype in a wide variety of central nervous system processes.

The light microscopic appearance of m3 suggests that this receptor may be compartmentalized in subcellular sites. For example, immunoreactivity in somata and proximal dendrites of neurons is consistent with postsynaptic distributions. The diffuse or punctate appearance of the immunoreactivity, as occurs in the molecular layer of cortex, hippocampus, striatum and many thalamic nuclei, is consistent with either presynaptic localization in terminals or postsynaptic localization in dendritic spines. In structures with little or no intrinsic expression of m3 mRNA, such as striatum,[3] presynaptic localization in the terminals of extrinsic afferent fibers may be more likely. In fact, we have recently confirmed the presynaptic localization of m3 in striatum by direct observation using immunoelecton microscopy.[10] Presynaptic muscarinic receptors, with M3-like binding preferences, regulate neurotransmitter release in striatum, as well as in hippocampus and amygdala.[20,29,32] Localization of m3 immunoreactivity at the ultrastructural level will be important to identify the pre- and postsynaptic distribution of this subtype in other regions.

Although presynaptic muscarinic receptor subtypes are well known to regulate the release of acetylcholine,[12,20,23,27,28,33] the molecular identity of the autoreceptor(s) in many brain regions is unknown. Several pharmacological and lesion studies have implicated M2 as an inhibitory presynaptic site modulating acetylcholine release in cortex, hippocampus and striatum.[12,21,23,28] The m2 protein may correspond to some of these binding sites, since the mRNA[3] and protein[16] are expressed at high levels in basal forebrain and in cholinergic neurons in striatum.[1,10] Moreover, immunoelectron microscopic studies have directly localized m2 protein to presynaptic sites which are likely to be cholinergic in necortex[24] and striatum.[10] Other subtypes may also be autoreceptors, since pharmacological studies have found that M1 sites in basal forebrain[33] and M3 sites in hippocampus[20] inhibit acetylcholine release. M1 sites in cortex stimulate release as well.[27] The m3 protein is a candidate for a muscarinic autoreceptor in cortex and hippocampus on both pharmacological and anatomical grounds. That is, its intermediate binding affinities for selective compounds are compatible with the varied pharmacologies reported for autoreceptors. The m3 mRNA[13] and, as shown here, the m3 protein are expressed in basal forebrain neurons which may project to cortex and hippocampus. However, the basal forebrain consists of heterogeneous cell populations, and whether m3 is expressed in the cholinergic neurons and also transported to terminal sites is unknown. Future studies to co-localize each receptor protein in cholinergic nerve terminals will be useful to clarify the molecular identity of the autoreceptors.

Despite the widespread distribution of m3, localization of this receptor suggests that it may play a special role in limbic processes. For example, among cortical areas, the limbic regions display the most intense m3 immunoreactivity, including cingulate, retrosplenial, entorhinal, insular and piriform cortex. Also, the hippocampus and amygdala are enriched in m3. Moreover, the limbic nuclei in the anterior thalamus, and the connectionally related neurons in the mammillary nuclei and posterior hypothalamus exhibit dense m3 immunoreactivity. Interestingly, many of these structures have been implicated in memory processes, and the diencephalic nuclei are also important in behavioral state control. A role for m3 in these cholinergic functions may have important clinical implications for targeting subtype-specific drugs in patients with memory and sleep disorders.

Are m3 and M3 the same receptor?

The immunocytochemical distribution of m3 was widespread in rat brain and generally consistent with the autoradiographic localization of M3. The most striking similarities were noted in deep endopiriform and insular cortex, striatum, anterior thalamic nuclei, superior colliculus, periaqueductal gray and pontine nuclei. These results corroborate predictions made previously by Zubieta and Frey.[43] who selected these structures as the regions in which the labeled sites are most likely to correspond to m3 protein. As discussed by these authors previously, sites labeled by [^{3}H]4-DAMP in the presence of pirenzepine and AF-DX 116 are predicted to include residual m1, m2 and m4 receptors in regions where these proteins are substantially higher than m3. However, those sites with the most enriched [^{3}H]4-DAMP binding, as determined by the ratio of residual binding in the presence or absence of the antagonists to block non-M3 receptors, are most likely to reflect m3. The correspondence of the markers in the aforementioned regions provides evidence that ligand binding sites labeled by these conditions are comprised mainly of m3 protein.

There are also notable differences in the distributions of m3 immunoreactivity and M3 binding sites in key regions and lamina of cortex and hippo-

campus. There are several possible explanations for these discrepancies. First, each probe may gain access to different populations of m3 receptors. Ligand binding is believed to reside within the transmembrane domains,[11] while the antibodies react with the putative third cytoplasmic loop.[16] Thus, ligands may bind to receptors in which the antibody binding sites are unavailable, e.g. due to post-translational modifications or interactions with other membrane proteins. Similarly, antibodies may detect receptors in synthetic or degradative pathways, or other discrete subcellular compartments in which the proteins are not functional or capable of binding ligands. A second factor possibly contributing to areas of mismatch is that M3 binding patterns have not been corrected for tritium quenching. This is a non-uniform process and results in an apparent reduction of isotope content in white matter. Thirdly, potential problems with the specificity of either probe may also add to differences between m3 and M3. As discussed above, this is a recognized problem for M3 binding, since even in the presence of pirenzepine and AF-DX 116 residual binding to other subtypes is expected.[43] Residual binding of [^{3}H]4-DAMP to m1 could in part explain the mismatch between m3 and M3 in both cortex and hippocampus, since m1 is abundant in these structures and the regional and laminar patterns of M3 binding appears nearly identical to that of m1.[16] Because m3 is present at low levels and barely detectable with our antibodies, we also cannot entirely exclude the possibility that m3 antibodies may cross-react with other brain proteins, despite their characterization by immunoprecipitation[16] and Western blotting analysis.[10] Regardless of the explanation, the m3/M3 mismatch in cortex and hippocampus suggests that m3 protein and M3 binding sites labeled with these conditions are not entirely equivalent.

A correspondence between the m3 gene/protein and the M3 binding site defined pharmacologically has been suggested in several important reviews,[8,11,22] and such a relationship is implicit in nomenclature recommended by the IUPHAR muscarinic committee.[39] Using the most selective probes available for both the m3 protein and the M3 binding site, we have shown that the markers may overlap, but imprecisely. Other pharmacologically defined sites are also likely to be composites of multiple receptor proteins given the well recognized problems with limited selectivity of available ligands[4,6,35] and the presence of multiple receptor proteins in most brain regions[16,42] and peripheral tissues.[5] For these reasons, we recommend that investigators use strict definitions for molecular (m1–m5) and pharmacological (M1–M4) classifications. Although reconciliation of dual classification systems would be ideal, until direct evidence proves otherwise, identities between these schemes should not be presumed.

CONCLUSIONS

The present study demonstrates that m3 receptor protein is present at low but measurable levels throughout discrete neuronal populations in the forebrain and upper brainstem. There is a close but imprecise relationship between m3 receptor detected by antibodies and M3 receptor detected by ligand autoradiography, suggesting that molecular and pharmacological classification schemes are not equivalent. However, because of the limitations inherent to each technique and the low abundance of this subtype, the receptors can be localized with the greatest certainty to structures that show agreement between m3 immunoreactivity and M3 binding. These structures include several limbic regions of cortex and thalamus, striatum, superior colliculus and pontine nuclei. This distribution suggests that m3/M3 mediates a variety of cholinergic functions, including possible roles in learning, memory, and motor and behavioral state control, and that this subtype is potentially a valuable target for therapeutic drugs for a variety of neurological and psychiatric disorders.

Acknowledgements—This work was supported by NS30454 (A.I.L.), P01 MH42652 (K.A.F.) and the American Parkinson's Disease Association Center of Excellence at Emory University. The authors thank Drs David Rye and Steven Hersch for helpful discussions and review of the manuscript.

REFERENCES

1. Bernard V., Normand E. and Bloch B. (1992) Phenotypical characterization of the rat striatal neurons expressing muscarinic receptor genes. *J. Neurosci.* **12,** 3591–3600.
2. Bonner T. I., Buckley N. J., Young A. C. and Brann M. R. (1987) Identification of a family of muscarinic acetylcholine receptor genes. *Science* **237,** 527–532.
3. Buckley N. J., Bonner T. I. and Brann M. R. (1988) Localization of a family of muscarinic receptor mRNAs in rat brain. *J. Neurosci.* **8,** 4646–4652.
4. Buckley N. J., Bonner T. I., Buckley C. M. and Brann M. R. (1989) Antagonist binding properties of five cloned muscarinic receptors expressed in CHO-K1 cells. *Molec. Pharmac.* **35,** 469–476.
5. Dorje F., Levey A. I. and Brann M. R. (1991) Immunological detection of muscarinic receptor subtype proteins (m1–m5) in rabbit peripheral tissues. *Molec. Pharmac.* **40,** 459–462.
6. Dorje F., Wess J., Lambrecht G., Tacke R., Mutschler E. and Brann M. R. (1991) Antagonist binding profiles of five cloned human muscarinic receptor subtypes. *J. Pharmac. exp. Ther.* **256,** 727–733.
7. Fisher S. K. and Snider R. M. (1987) Differential receptor occupancy requirements for muscarinic cholinergic stimulation of inositol lipid hydrolysis in brain and in neuroblastomas. *Molec. Pharmac.* **32,** 81–90.

8. Goyal R. K. (1989) Muscarinic receptor subtypes: physiology and clinical implications. *New Engl. J. Med.* **321,** 1022–1029.
9. Hammer R., Berrie C. P., Birdsall N. J. M., Burgen A. S. V. and Hulme E. C. (1980) Pirenzepine distinguishes between subclasses of muscarinic receptors. *Nature* **283,** 90–92.
10. Hersch S. M., Gutekunst C. A., Rees H. D., Heilman C. J. and Levey A. I. (1994) Distribution of m1–m4 muscarinic receptor proteins in the rat striatum: light and electron microscopic immunocytochemistry using subtype-specific antibodies. *J. Neurosci.* **14,** 3351–3363.
11. Hulme E. C., Birdsall N. J. M. and Buckley N. J. (1990) Muscarinic receptor subtypes. *A. Rev. Pharmac. Toxic.* **30,** 633–673.
12. Lapchak P. A., Araujo D. M., Quirion R. and Collier B. (1989) Binding sites for [^{3}H]AF-DX 116 and effect of AF-DX 116 on endogenous acetylcholine release from rat brain slices. *Brain Res.* **496,** 285–294.
13. Levey A., Weiner D. and Brann M. R. (1990) Molecular identification of central cholinergic autoreceptors. *Fedn Proc. Fedn Am. Socs exp. Biol.* **4,** A1914–A1910 (Abstract).
14. Levey A. I., Armstrong D. M., Atweh S. F., Terry R. D. and Wainer B. H. (1983) Monoclonal antibodies to choline acetyltransferase: production, specificity, and immunohistochemistry. *J. Neurosci.* **3,** 1–9.
15. Levey A. I., Hersch S. M., Rye D. B., Sunahara R., Niznik H., Kitt C. A., Price D. L., Maggio R., Brann M. R. and Ciliax B. J. (1993) Localization of D1 and D2 dopamine receptors in rat, monkey, and human brain with subtype-specific antibodies. *Proc. natn. Acad. Sci. U.S.A.* **90,** 8861–8865.
16. Levey A. I., Kitt C. A., Simonds W. F., Price D. L. and Brann M. R. (1991) Identification and localization of muscarinic acetylcholine receptor proteins in brain with subtype-specific antibodies. *J. Neurosci.* **11,** 3218–3226.
17. Levey A. I., Stormann T. M. and Brann M. R. (1990) Bacterial expression of human muscarinic receptor fusion proteins and generation of subtype-specific antisera. *Fedn Eur. biochem. Socs Lett.* **275,** 65–69.
18. Li M., Yasuda R. P., Wall S. J., Wellstein A. and Wolfe B. B. (1991) Distribution of m2 muscarinic receptors in rat brain using antisera selective for m2 receptors. *Molec. Pharmac.* **40,** 28–35.
19. Luthin G. R., Harkness J., Artymyshyn R. P. and Wolfe B. B. (1988) Antibodies to a synthetic peptide can be used to distinguish between muscarinic acetylcholine receptor binding sites in brain and heart. *Molec. Pharmac.* **34,** 327–333.
20. Marchi M. and Raiteri M. (1989) Interaction of acetylcholine–glutamate in rat hippocampus: involvement of the two subtypes of M-2 muscarinic receptors. *J. Pharmac. exp. Ther.* **248,** 1255–1260.
21. Mash D. C., Flynn D. D. and Potter L. T. (1985) Loss of M2 muscarine receptors in the cerebral cortex in Alzheimer's disease and experimental cholinergic denervation. *Science* **228,** 1115–1117.
22. McKinney M. and Coyle J. T. (1991) The potential for muscarinic receptor subtype-specific pharmacotherapy for Alzheimer's disease. *Mayo Clin. Proc.* **66,** 1225–1237.
23. Meyer E. M. and Otero D. H. (1985) Pharmacological and ionic characterizations of the muscarinic receptors modulating [^{3}H]acetylcholine release from rat cortical synaptosomes. *J. Neurosci.* **5,** 1202–1207.
24. Mrzljak L., Levey A. I. and Goldman-Rakic P. S. (1993) Association of m1 and m2 muscarinic receptor proteins with asymmetric synapses in the primate cerebral cortex: morphological evidence for cholinergic modulation of excitatory neurotransmission. *Proc. natn. Acad. Sci. U.S.A.* **90,** 5194–5198.
25. Munson P. J. and Rodbard D. (1980) Ligand: a versatile computerized approach for the characterization of ligand binding systems. *Analyt. Biochem.* **107,** 220–239.
26. Peralta E. G., Ashkenazi A., Winslow J. W., Smith D. H., Ramachandran J. and Capon D. J. (1987) Distinct primary structures, ligand-binding properties and tissue-specific expression of four human muscarinic acetylcholine receptors. *Eur. molec. Biol. Org. J.* **6,** 3923–3929.
27. Pittel Z., Heldman E., Rubenstein R. and Cohen S. (1990) Distinct muscarinic receptor subtypes differentially modulate acetylcholine release from corticocerebral synaptosomes. *J. Neurochem.* **55,** 665–672.
28. Raiteri M., Leardi R. and Marchi M. (1984) Heterogeneity of presynaptic muscarinic receptors regulating neurotransmitter release in the rat brain. *J. Pharmac. exp. Ther.* **228,** 209–214.
29. Raiteri M., Marchi M., Paudice P. and Pittaluga A. (1990) Muscarinic receptors mediating inhibition of gamma-aminobutyric acid release in rat corpus striatum and their pharmacological characterization. *J. Pharmac. exp. Ther.* **254,** 496–501.
30. Sakamoto S., Goto S., Ito H. and Hirano A. (1992) Striosomal organization of substance P-like immunoreactivity in parkinsonian patients. *Neurology* **42,** 1071–1075.
31. Smith P. K., Krohn R. I., Hermanson G. T., Mallia A. K., Gartner F. H., Provenzano M. D., Fujimoto E. K., Goeke N. M., Olson B. J. and Klenk D. C. (1985) Measurement of protein using bicinchoninic acid. *Analyt. Biochem.* **150,** 76–85.
32. Sugita S., Uchimura N., Jiang Z.-G. and North R. A. (1991) Distinct muscarinic receptors inhibit release of gamma-aminobutyric acid and excitatory amino acids in mammalian brain. *Proc. natn. Acad. Sci. U.S.A.* **88,** 2608–2611.
33. Suzuki T., Fujimoto K., Oohata H. and Kawashima K. (1988) Presynaptic M1 muscarinic receptor modulates spontaneous release of acetylcholine from rat basal forebrain slices. *Neurosci. Lett.* **84,** 209–212.
34. Vilaro M. T., Palacios J. M. and Mengod G. (1990) Localization of m5 muscarinic receptor mRNA in rat brain examined by *in situ* hybridization histochemistry. *Neurosci. Lett.* **114,** 154–159.
35. Vilaro M. T., Wiederhold K. H., Palacios J. M. and Mengod G. (1992) Muscarinic M2-selective ligands also recognize M4 receptors in the rat brain: evidence from combined *in situ* hybridization and receptor autoradiography. *Synapse* **11,** 171–183.
36. Waelbroeck M., Tastenoy M., Camus J. and Christophe J. (1990) Binding of selective antagonists to 4 muscarinic receptors (M1 to M4) in rat forebrain. *Molec. Pharmac.* **38,** 267–273.
37. Wall S. J., Yasuda R. P., Hory F., Flagg S., Martin B. M., Ginns E. I. and Wolfe B. B. (1991) Production of antisera selective for m1 muscarinic receptors using fusion proteins: distribution of m1 receptors in rat brain. *Molec. Pharmac.* **39,** 643–649.
38. Wall S. J., Yasuda R. P., Li M. and Wolfe B. B. (1991) Development of an antiserum against m3 muscarinic receptors: distribution of m3 receptors in rat tissues and clonal cell lines. *Molec. Pharmac.* **40,** 783–789.
39. Watson S. W. and Girdlestone D. (1993) TIPS receptor nomenclature supplement. *Trends pharmac. Sci.* 25.

40. Wei J., Milici A. and Buccafusco J. J. (1993) m1–m5 muscarinic receptor distribution and quantitation in rat CNS by RT-PCR and HPLC. *Soc. Neurosci. Abstr.* **19,** 1130 (Abstract).
41. Weiner D. M., Levey A. I. and Brann M. R. (1990) Expression of muscarinic acetylcholine and dopamine receptor mRNAs in rat basal ganglia. *Proc. natn. Acad. Sci. U.S.A.* **87,** 7050–7054.
42. Yasuda R. P., Ciesla W., Flores L. R., Wall S. J., Li M., Satkus S. A., Weisstein J. S., Spagnola B. V. and Wolfe B. B. (1993) Development of antisera selective for m4 and m5 muscarinic cholinergic receptors: distribution of m4 and m5 receptors in rat brain. *Molec. Pharmac.* **43,** 149–157.
43. Zubieta J. K. and Frey K. A. (1993) Autoradiographic mapping of M3 muscarinic receptors in the rat brain. *J. Pharmac. exp. Ther.* **264,** 415–422.

(*Accepted* 25 *May* 1994)